International Journal of Architectural, Civil and Construction Sciences
ISSN: 2415-1734
Vol:5, No:8, 2011

Effect of the Rise/Span Ratio of a Spherical Cap Shell on the Buckling Load

Peter N. Khakina, Mohammed I. Ali, Enchun Zhu, Huazhang Zhou and Baydaa H. Moula

Abstract**—**Rise/span ratio has been mentioned as one of the reasons which contribute to the lower buckling load as compared to the Classical theory buckling load but this ratio has not been quantified in the equation. The purpose of this study was to determine a more realistic buckling load by quantifying the effect of the rise/span ratio because experiments have shown that the Classical theory overestimates the load. The buckling load equation was derived based on the theorem of work done and strain energy. Thereafter, finite element modeling and simulation using ABAQUS was done to determine the variables that determine the constant in the derived equation. The rise/span was found to be the determining factor of the constant in the buckling load equation. The derived buckling load correlates closely to the load obtained from experiments.

Keywords**—**Buckling, Finite element, Rise/span ratio, Spherical cap

I.INTRODUCTION

THIN spherical shells are efficient and economical. The load-carrying capability of these structures is usually dominated by buckling thus the need to accurately predict the buckling load. Experimental studies have shown that the buckling load of shells is usually overestimated by the classical buckling theory [1]. Factors which contribute to this overestimation include: a) Geometric parameters b) material parameters c) boundary conditions d) pre-buckling deformations and e) geometric imperfections [2]. It is difficult to quantify the geometric imperfections because they are introduced during construction but the geometrical parameters can be quantified because they are decided upon before construction. One of the geometrical parameters is the rise/span (f/L) ratio. Little has been done to quantify the effect of f/L ratio to the buckling load because most researchers use the Classical theory as their base for determining the load, which is based on a complete spherical shell. However, most wide roof constructions are in the form of spherical cap which has a rise (f) and a span (L). According to classical buckling theory, the critical value of the membrane stress is as stated in [3]:

$$q_{cr} = \frac{Et}{\sqrt{3\left(1-\nu^2\right)}R} \tag{1}$$

thus the buckling load is:

$$q_{cr} = \frac{2E}{\sqrt{3\left(1-\nu^2\right)}}\left(\frac{t}{R}\right)^2 \tag{2}$$

where; q_{cr} is the critical buckling load in the form of radial pressure, σ_{cr} the critical buckling stress, R is the radius of curvature, t the thickness of the shell wall, E the Young's modulus and ν the Poisson's ratio of the material.

Prevost *et al* [4], mentions that the buckling load can be expressed in the form:

$$q_{cr} = CE\left(\frac{t}{R}\right)^{\alpha} \tag{3}$$

where, q_{cr} is the critical buckling load, t it the thickness of the shell, R is its radius of curvature, E is the Modulus of elasticity of the material and C and α are constants which are to be determined. As mentioned in [5], α is given the value 2 but the equation for C is yet to be determined. Some researchers have assumed that the f/L ratio is taken into consideration when calculating the radius of curvature (R) but R can be constant and different buckling loads obtained with varying f/L ratio. In this study, the effect of geometrical imperfections is eliminated by using the post-buckling load so that the constant C remains to be a function of f/L ratio. The post-buckling load is observed from the 'plateau' on the load-deflection curves. The plateau is formed irrespective of the initial geometrical imperfection. Also the theorem of work done and the stain energy is used to determine the value of α.

II.EMPIRICAL PREDICTIONS OF BUCKLING LOAD OF THIN SPHERICAL SHELLS

When a concentrated load is applied at the apex of a spherical cap, the shell deforms in a shape as shown in Fig. 1. The magnitude of r as compared to R is usually very small making α to be also very small.

From Fig. 1:

$$r = R\sin\alpha \approx R\alpha \tag{4}$$

The depth of buckling:

$$w_o = 2R\left(1-\cos\alpha\right) \quad R\sin^2\frac{\alpha}{2} = \tag{5}$$

School of Civil Engineering, Harbin Institute of Technology, 2453 P.O. BOX 73, Huanghe Road, Harbin 150090, China. Corresponding author phone
e-mail: nyongpet@yahoo.com

Since α is very small, it may be assumed that:

$$w_0 \approx R\alpha^2 \tag{6}$$

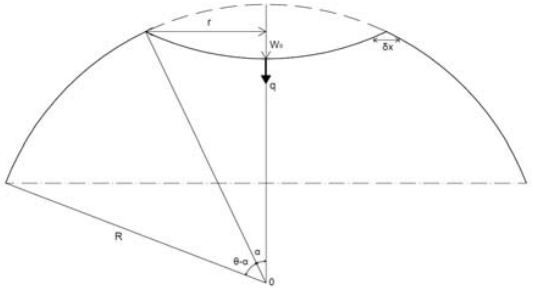

Fig. 1 Inversion of spherical shell by a concentrated force

The work done is given by the product of the concentrated force (q) and the volume of the inversed region:

$$W = \frac{4}{3}\pi q r^2 \left(\frac{w_o}{2}\right) \tag{7}$$

Substituting (4) and (6) into (7):

$$W = \frac{2}{3}\pi\alpha q r^3 \tag{8}$$

The strain energy is concentrated along the boundary layer of the inversed region as shown in Fig. 2. The total strain energy as given by [6] is:

$$U = Er^3\left(\frac{t}{R}\right)^{2.5} \tag{9}$$

The work done for the inversion of the shell is the same as the strain energy according to work-energy method [7]. This implies that (8) and (9) should be equal. Equating the two equations:

$$\frac{2}{3}\pi\alpha q r^3 = Er^3\left(\frac{t}{R}\right)^{2.5} \tag{10}$$

Solving for q:

$$q = \frac{3E}{2\pi\alpha}\left(\frac{t}{R}\right)^{2.5} \tag{11}$$

Since the value of α in Fig. 1 is not known, we introduce a constant C so as to express it in relation to f/L ratio because it is this ratio that determines the value of α. Therefore, it can be finalized that:

$$q_{cr} = CE\left(\frac{t}{R}\right)^{2.5} \tag{12}$$

where, C is a constant.

III.FINITE ELEMENT MODELING TO DETERMINE THE VALUE OF C

3.1 Post-Buckling Load

Using Finite Element (FE) analysis produces the optimum product; a product that is the least costly to produce, performs as intended and meets all of the specified requirements [8]. Also, the structural behavior of shell structures during the whole loading process can be revealed by the load-deflection curves and the buckling load can be predicted with sufficient accuracy [9].

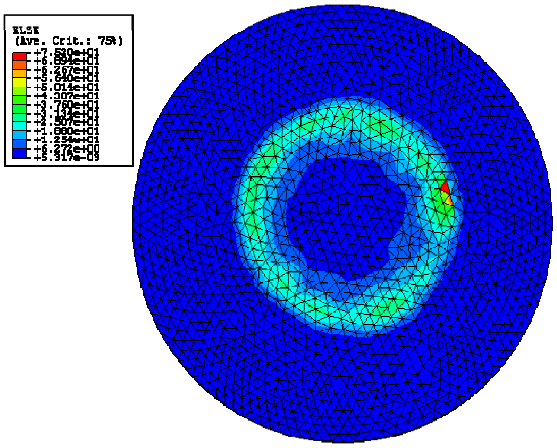

Fig. 2 Concentration of strain energy

Maximum load that a structure can safely carry can be calculated by performing an incremental analysis using the non-linear formulation. Therefore FE modeling was done on several shells to find out the effect of f/L ratio on the buckling load. Steel being a very good material for construction of shells, a mild steel spherical cap shell of E = 200 x 10^9 N/m^2 and Poisson Ratio (ν) = 0.3, L= 20m and t=0.02m was initially used for the modeling. The initial geometry of the spherical cap shell is shown in Fig. 3. Initial geometrical imperfection was introduced by a dimple as shown in Fig. 4. During construction, initial geometrical imperfections may be introduced due to imperfect spherical shape resulting in uneven curvature. Using ABAQUS, the shell was meshed with triangular shell elements-S3R [10] with a typical side length of 500mm. Riks method [11] was used to trace the load-deflection curves which are shown in Fig. 5.

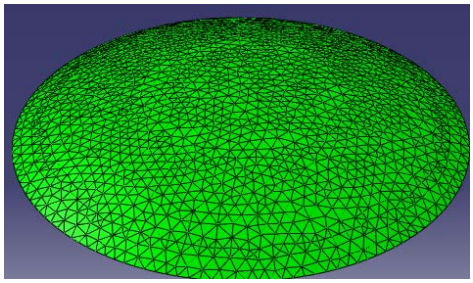

Fig. 3 Geometry of the spherical cap shell

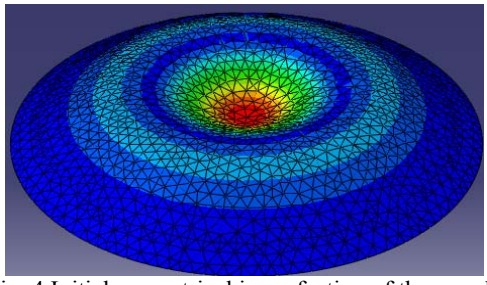

Fig. 4 Initial geometrical imperfection of the cap shell

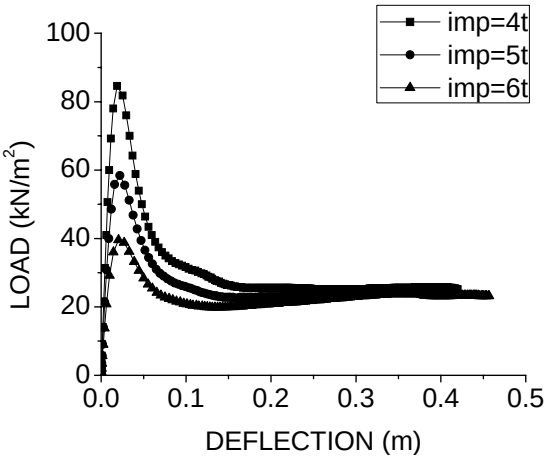

Fig. 5 Load-deflection curves of different magnitudes of initial geometrical imperfections for f/L = 1/8.

We observed from Fig. 5 that the initial buckling of the shell is sensitive to the initial geometrical imperfection as also observed by [12] while the post-buckling load is little influenced because irrespective of the magnitude of the imperfection, the curves tend to meet at the 'plateau'. Therefore using the post-buckling load eliminates the effect of geometrical imperfections.

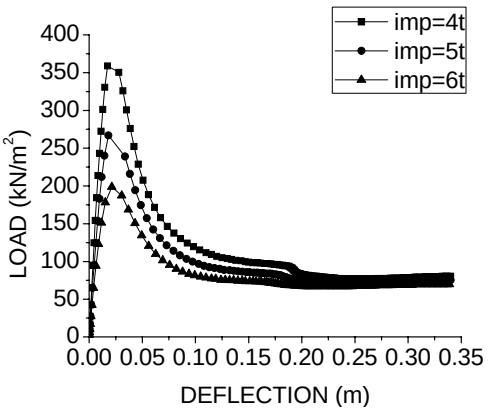

Fig. 6 Load-deflection curves of different magnitudes of initial geometrical imperfections for f/L = 1/4.

3.2 Test for the Effect of f/L Ratio

While keeping L, t and other factors constant, different f/L ratios were modeled and simulated. We observed that the load-deflection curves in every ratio formed a 'plateau' at the post buckling load. The load-deflection curves are shown in figures 6 - 8.

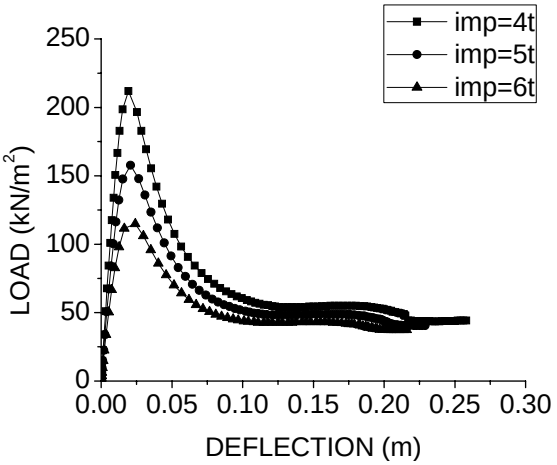

Fig. 7 Load-deflection curves of different magnitudes of initial geometrical imperfections for f/L = 1/6

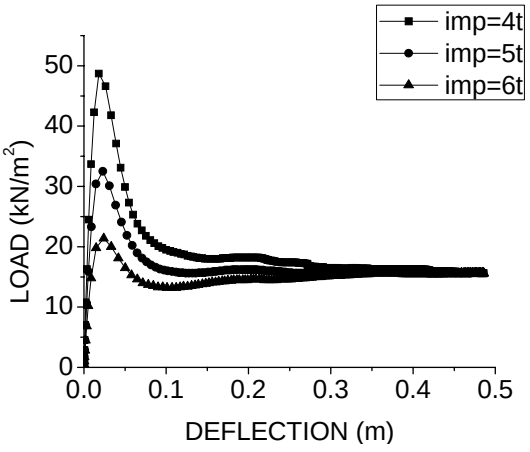

Fig. 8 Load-deflection curves of different magnitudes of initial geometrical imperfections for f/L = 1/10

The load-deflection curve from each ratio which had an average value of the post-buckling load was used to draw the curves in Fig. 9.

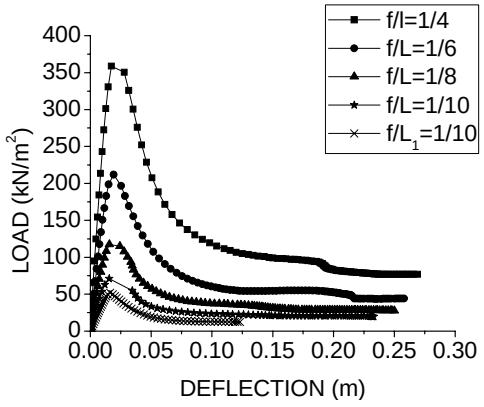

Fig. 9 Load-deflection curves for varying f/L and with other factors remaining constant

From the load-deflection curves shown in Fig. 9, the values of C based on (12) are calculated and shown in table 1.

TABLE I
VALUES OF C WITH DIFFERENT F/L RATIOS

f/L	L (m)	t (m)	Post-buckling load (kN/m^2)	Value of C
1/4	20	0.02	77.00	3.76
1/6	20	0.02	45.97	4.61
1/8	20	0.02	28.91	5.32
1/10	20	0.02	19.53	5.95
1/10	30	0.02	12.29	10.32

We observed as seen in table 1 that the constant C is inversely proportional to f/L ratio. However, the relationship is not linear making it necessary to determine the indices of the geometrical parameters. Two unknowns (x and y) are introduced as indices as to represent the relationship as:

$$\frac{1}{C} \propto \frac{f^x}{L^y} \tag{13}$$

Introducing the constant of proportionality:

$$C = k\frac{L^y}{f^x} \tag{14}$$

Rearranging:

$$Cf^x = kL^y$$

Introducing logs on both sides:

$$\log C + x\log f = \log k + y\log L \tag{15}$$

Substituting in (15) the values for f/L = 1/4 in table 1:

$$\log 3.76 + x\log 5 = \log k + y\log 20$$

Rearranging:

$$\log k + 1.301y - 0.699x = 0.575 \tag{16}$$

Substituting in (15) the values for f/L =1/10 for L = 20m in table 1:

$$\log 5.95 + x\log 2 = \log k + y\log 20$$

Rearranging:

$$\log k + 1.301y - 0.301x = 0.7745 \tag{17}$$

Subtracting (16) from (17):

$$0.398x = 0.1995$$

Solving for x:

$$x = 0.5$$

Substituting the value of x in (16) and solving:

$$\log k + 1.301y = 0.9245 \tag{18}$$

Substituting in (15) the values for f/L = 1/10 for L = 30m in table 1:

$$\log 10.32 + x\log 3 = \log k + y\log 30$$

Substituting for x and rearranging:

$$\log k + 1.477y = 1.2526 \tag{19}$$

Subtracting (18) from (19):

$$0.176y = 0.3281$$

Solving for y:

$$y = 1.86$$

Substituting the value of y in (19) and solving for k:

$$k = 0.032$$

Therefore:

$$C = 0.032\frac{L^{1.86}}{f^{0.5}} \tag{20}$$

Equation (18) is valid for all f/L as seen in table I.

3.3 Effect of the f/L Ratio on the Buckling Load

It is clearly shown that the initial buckling of the shell is sensitive to the initial geometrical imperfection while the post-buckling behavior is little influenced because the curves tend to meet at the post-buckling load. Therefore using the post-buckling load eliminates the effect of all types of imperfections. Boundary conditions have little influence on buckling [13] and the effect of pre-buckling deformations is very small if any according to [14]. Therefore C can be assumed to be mainly a function of the f/L ratio. The study shows that the effect of f/L which is inversely proportional to the Constant C. It can therefore be concluded that the critical buckling load of a spherical cap shell is given by:

$$q_{cr} = CE\left(\frac{t}{R}\right)^{2.5}$$

Substituting for C:

$$q_{cr} = \frac{0.032EL^{1.86}}{f^{0.5}}\left(\frac{t}{R}\right)^{2.5} \quad (21)$$

where, q_{cr} is the critical buckling load, t it the thickness of the shell, R is its radius of curvature, f is the rise of the spherical cap shell, L is the span of the shell and E is the Modulus of elasticity of the material.

IV. VALIDATION OF THE DERIVED BUCKLING LOAD

To validate the derived equation, shells with different geometrical parameters were modeled and simulated. Various spans, rises and thicknesses were used to test whether the derived formula was valid for different geometrical parameters. The load-deflection curves are shown in figures 10 – 14.

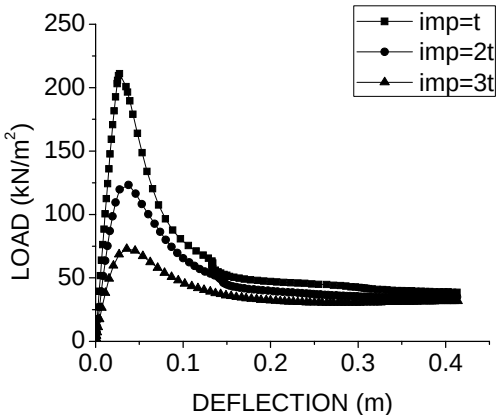

Fig. 10 Load-deflection curves, L = 30m, f = 3m and t = 0.04m

Other factors were kept constant as in section 3.1. The load-deflection curves from different shells, which had values equal to the average of the post-buckling load at the 'plateau', are shown on the same axes in Fig. 15. The values from the derived formula are compared with results from FE modeling based on the post-buckling load. Also the values are compared to the Classical buckling theory load in terms of percentages as shown in table II.

The values for the critical buckling load from the derived formula and from FE modeling are almost the same showing that the formula is valid. Theoretical results by many researchers range approximately from 7 to 67% of the classical buckling load [15]. The derived formula gives a buckling load whose percentage (as compared to that of the Classical buckling theory) is within the range. This also confirms that the formula is valid as compared to what other researchers have done.

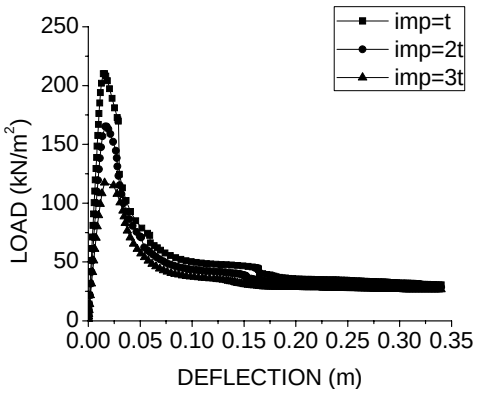

Fig. 11 Load-deflection curves, L = 20m, f = 2.5m and t = 0.02m.

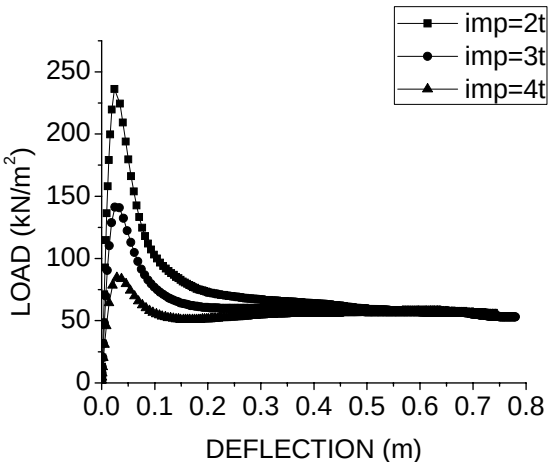

Fig. 12 Load-deflection curves, L = 20m, f = 2.5m and t = 0.02m.

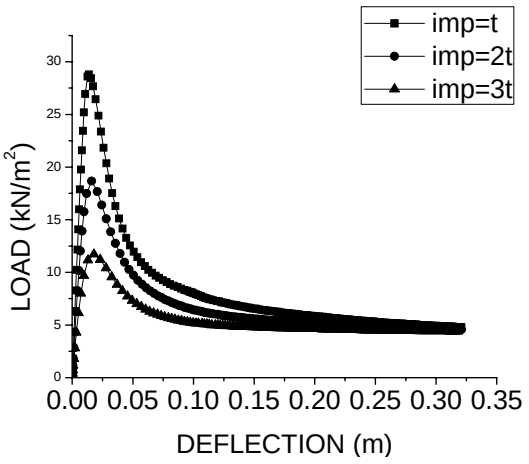

Fig. 13 Load-deflection curves, L = 20m, f = 1m and t = 0.02m.

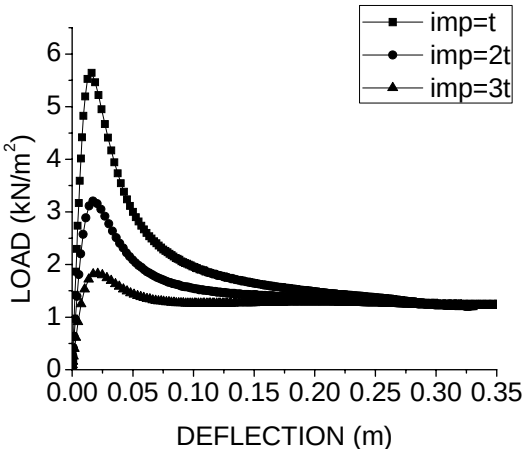

Fig. 14 Load-deflection curves, L = 20m, f = 0.5m and t = 0.02m.

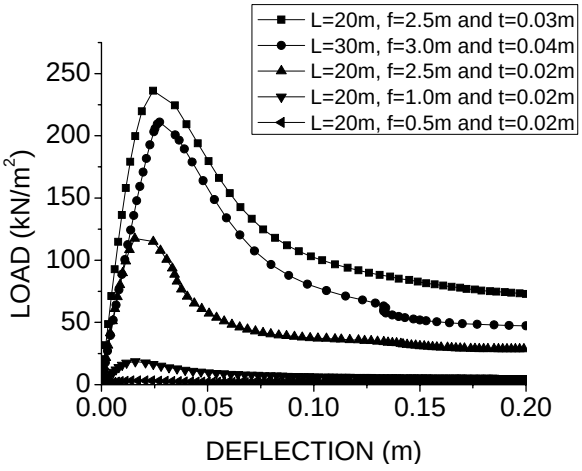

Fig. 15 Load-deflection curves for different shells

V.CONCLUSIONS

The Classical buckling theory does not consider the f/L ratio of the shell because a complete spherical shell was used to determine the membrane stresses. Researchers have used this theory to predict the buckling load of spherical shells due to fact that the stresses are the same as those of the complete shell but they just mention f/L ratio as a contributing factor to the lower buckling load. In this study, f/L ratio has been quantified so as to give a more realistic critical buckling load. The constant C has been determined mathematically with the help of FE modeling. The empirical prediction of the buckling load has also shown that the buckling load is proportional to $t^{2.5}$, which gives the value of α as 2.5. This proportionality was also observed by [16] for cylindrical shells. We observed that the rise/span ratio has an effect of lowering the buckling load as compared the prediction of the Classical theory because increasing L also affects R. Further work can be done to use the derived formula to predict the buckling load of single-layer reticulated shells using the continuum analogy method because according to [17], it is possible to find a statically equivalent continuum and reduce the overall stability analysis of a grid structure to that of a continuous shell.

TABLE II
VALIDATION OF DERIVED FORMULA

Shell	Geometrical parameters in metres			Buckling load by the derived formula (kN/m^2)	Buckling load from the FE modeling (kN/m^2)	Classical buckling theory load (kN/m^2)	Derived formula value Percentage (%) of Classical load
	L	**f**	**t**				
1	20	2.5	0.03	79.71	79.65	482.51	17
2	30	3.0	0.04	69.59	69.62	254.67	27
3	20	2.5	0.02	28.93	29.45	214.45	14
4	20	1.0	0.02	5.25	5.26	37.97	14
5	20	0.5	0.02	1.34	1.34	9.64	14

REFERENCES

[1] E. C. Zhu, Z. W. Guan, P. D. Rodd and D. J. Pope, "Buckling of Oriented Strand Board Webbed Wood I-Joists", J. Struct Eng., vol 131(10), 2005, pp. 629-1636.
[2] G. Forasassi and R. Frano, "Curved thin shell buckling behavior", J. Achievements in Materials and Manufacturing Eng., Vol. 23(2), 2007, pp. 55-58.
[3] S. P. Timoshenko and J.M. Gere, "Theory of elastic stability". London: McGraw-Hill Book Company; 1963.
[4] J. H. Prevost, D. P. Billington, R. Rowland and C. C. LIM, "Buckling of Spherical dome in a centrifuge", Exp. Mech., 1984, pp. 203-207.
[5] S. Narayanan, Space structures: Principles and practice. Brentwood: Multi-Science publishing Co. Ltd, 2006.
[6] L. D. Landau and E. M. Lifshitz, "Theory of Elasticity". Oxford: Butterworth-Heinemann, 1986.
[7] L. Xifu, Z. Tao and Z. Chunxiang, "Theoretical Mechanics". Harbin: Harbin Institute of Technology press, 2007.
[8] E. R. Champion, "Finite Element Analysis in manufacturing Engineering: APC– Based approach". New York: McGraw-Hill, Inc., 1992.
[9] F. Fan, Z. Cao, and S. Shen, "Elasto-plastic stability of single-layer reticulated shells", Thin walled Struct. vol 48, 2010, pp. 827-836.
[10] Hibbit, Karlsson & Sorensen Inc. ABAQUS theory manual Version 6.1. 2000.
[11] Hibbit, Karlsson & Sorensen Inc. ABAQUS user's manual Version 6.1. 2000.
[12] H. Z. Zhou, F. Fan, E. C. Zhu, "Buckling of reticulated laminated veneer lumber shells in consideration of the creep", Eng. Struct. Vol 32, 2010, pp. 2912-18.
[13] M. Barski, "Optimal design of shells against buckling subjected to combined Loadings", Struct. Multidisc Optim. Vol 31, 2006, pp. 211-222.
[14] G. J. Teng, "Buckling of thin shells: Recent advances and trends", Appl. Mech. vol 49, 1996, pp. 263-274.
[15] C. Y. Chia, "Buckling of Thin Spherical Shells", Ingenieur-Archiv, vol 40, 1971, pp. 227-237.
[16] E. Zhu, P. Mandal and C. R. Calladine, "Buckling of thin cylindrical shells: An attempt to resolve a paradox", Int. J. Mech. Sci., vol 44, 2002, pp. 1583-601.
[17] L. Kollar and E. Dulacska, "Buckling of shells for engineers". London: John Willey & sons, 1884.